# First-principle study on anatase TiO$_2$ codoped with nitrogen and ytterbium*

Gao Pan(高攀)[1], Zhang Xuejun(张学军)[2], Zhou Wenfang(周文芳)[1], Wu Jing(吴晶)[1],
and Liu Qingju(柳清菊)[1,†]

*(1 Yunnan Key Laboratory of Nanomaterials & Technology, Yunnan University, Kunming 650091, China)*
*(2 Department of Physics and Electric Information Engineering, Hunan City University, Yiyang 413000, China)*

**Abstract:** Crystal structures, electronic structures and optical properties of nitrogen and ytterbium doping anatase TiO$_2$ were calculated by first principles with the plane-wave ultrasoft pseudopotential method based on the density functional theory. The calculated results show that the octahedral dipole moments in TiO$_2$ increase due to the changes in lattice parameters, bond length and charges on atoms, which is very effective for the separation of photoexcited electron-hole pairs and the improvement of the photocatalytic activity of TiO$_2$. The interband transition between OP$_\pi$ states and Yb4f states make nitrogen and ytterbium doped TiO$_2$ manifest greater absorption coefficients in the visible-light region.

## 1. Introduction

As a photocatalytic material, TiO$_2$, owning to its nontoxicity, low cost and chemical stability, has been used in many fields such as solar cells, air and water pollution control and self-cleaning. It is the most potential photocatalyst. However, as a wide band gap oxide semiconductor ($E_g$ = 3.23 eV), anatase TiO$_2$ only shows photocatalytic activity under UV-light irradiation ($\lambda$ < 384 nm) that accounts for only a small fraction ($\sim$5%) of the solar energy, so its solar energy utilization is very low. Furthermore, its photo quantum yield is also very low due to its photoexcited electron-hole pairs easily recombining. Therefore, narrowing the band gap and reducing the recombination rate of photoexcited electron–hole pairs are the effective measures needed to improve the photocatalytic activity of TiO$_2$. Recently, many attempts have been made to improve the photocatalytic performance of TiO$_2$ under visible-light irradiation, such as ion-doping[1−3], noble metal loading[4], semiconductor compounding[5] and dye sensitizing[6]. In these modification methods, ion doping is considered as one of the most effective methods.

In particular, because of the unique 4f electronic configuration and spectral characteristics, lanthanides are ideal dopants for modifying the crystal structure, electronic structure and optical properties of TiO$_2$. On the other hand, Np state hybrids with O2p states in anatase TiO$_2$, because their energies are very close, and thus the band gap of TiO$_2$ is narrowed and has the ability to absorb visible light. Previous research has mostly been concentrated on the single ion-doping into TiO$_2$[7,8], but some recent research has shown that compared with single ion-doping, different ions codoping into TiO$_2$ can further enhance its optical absorption scope and photocatalytic activity by the synergistic reaction. Xu *et al.*[9] Eu and N codoping TiO$_2$ nanoparticles shows that the codoped photocatalysts exhibit smaller spherical shape particles, the absorbance spectra

exhibit a significant red shift to the visible region, and the photocatalytic activity is highly improved compared to N-doped TiO$_2$, pure TiO$_2$. Liu *et al.*[10] synthesized the metal and nitrogen codoping TiO$_2$ photocatalysts, they find that the codoping TiO$_2$ has a highly photoresponse for visible-light, and the radius and alterable valence states of doping metallic cations play important roles on their photocatalytic activity.

Experimental studies of ions codoping TiO$_2$ have achieved some results, but there are still many controversies on the modification mechanism of ion doping TiO$_2$ due to widely varying experimental conditions, sample preparations, the determination of photoreactivity, and the lack of detailed information about effects of ion doping on electronic structure of TiO$_2$. In contrast to experimental investigations, the theoretical analysis by computer simulation could overcome effects of complex experimental factors and clarify the ion doping effects on crystal structure and electronic structure[11−14].

In order to further investigate the modification mechanism of anatase TiO$_2$ doped with N and Yb, the plane-wave ultrasoft pseudopotential method within the framework of the first-principles has been used to calculate the crystal structure, electronic structure and optical properties of N+Yb-doped TiO$_2$, and compared them with that of N-doped, Yb-doped and pure TiO$_2$, in order to clarify how these ions impact the photocatalytic activity of TiO$_2$.

## 2. Calculation models and methods

Anatase TiO$_2$ has a tetragonal structure (space group: I4$_1$/amd, local symmetry: $D_{4h}^{19}$) and contains four Ti atoms and eight O atoms in the conventional cell. As shown in Fig. 1, our models (2 × 2 × 1 supercell) consisted of four conventional cells stacked along the a-axes and b-axes. In N+Yb-doped TiO$_2$ model, a Ti atom was substituted by a Yb atom and an O atom was substituted by a N atom. Thus, one supercell consisted of 15 Ti atoms, 31 O atoms, one Yb atom and one N atom.

Table 1. Formation energies, lattice distortions, average bond lengths, average net charges and average dipole moments of difficient ion doped $TiO_2$ by geometry optimization.

| | $E_f$ (eV) | Bond length (Å) | | | $\Delta V$ (Å$^3$) | Net charge (eV) | | | | Dipole moment (D) |
| | | Ti–O | Ti–N | Yb–O | | Ti | O | N | Yb | $TiO_6$ |
| --- | --- | --- | --- | --- | --- | --- | --- | --- | --- | --- |
| Pure $TiO_2$ | | 1.9326 | | | | 1.270 | −0.630 | | | 0.000 |
| N-doped | 2.062 | 1.9350 | 1.9654 | | 0.064 | 1.248 | −0.633 | −0.580 | | 0.030 |
| Yb-doped | 7.938 | 1.9375 | | 2.1174 | 0.802 | 1.247 | −0.626 | | 1.310 | 0.040 |
| N+Yb-doped | 9.809 | 1.9386 | 2.0074 | 2.1241 | 0.874 | 1.238 | −0.625 | −0.510 | 1.330 | 0.106 |
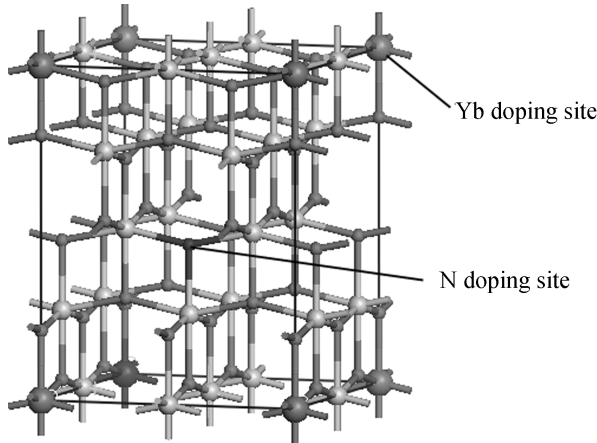


Fig. 1. Supercell model of N+Yb-doped anatase $TiO_2$ in the present word and the site of dopants.



Fig. 2. Calculated band structure of pure $TiO_2$.

The atomic concentration of impurity was about 2.08% (atomic fraction) in total. The other models are created by the same method.

All calculations are performed with the CASTEP module in Materials Studio 4.0 developed by Accelrys Software Inc. CASTEP is a first principle quantum mechanical process based on the density function theory (DFT). It uses a total energy plane-wave pseudopotential method. The wave functions of valence electrons are expanded using a plane-wave basis set within a specified energy cutoff that is chosen as 380 eV. The electronic exchange-correlation energy is treated within the framework of the local density approximation (LDA). The core electrons are replaced by the ultrasoft core potentials, and the valence atomic configurations are $3s^23p^63d^24s^2$ for Ti, $2s^22p^4$ for O, $2s^22p^3$ for N and $4f^{14}5s^25p^66s^2$ for Yb in the calculation. The Monkhorst–Pack scheme K-points grid sampling was set as $3 \times 7 \times 3$ for the irreducible Brilloium zone. A $45 \times 24 \times 54$ mesh was used for fast Fourier transformation. The convergences were set as $5 \times 10^{-4}$ Å for maximum displacement tolerances, 0.1 eV/nm for maximum force, 0.02 GPa for maximum stress and $5 \times 10^{-6}$ eV/atom for total energy change in the geometry optimization.

## 3. Results and discussion

### 3.1. Crystal structure

By optimizing the pure anatase $TiO_2$ supercell, we got the lattice parameters as follows: $a = b = 3.743$ Å, $c = 9.481$ Å, $d_{ap} = 1.970$ Å, $d_{eq} = 1.914$ Å, $2\theta = 155.840°$. They are in good agreement with the experimental results[15]: $a = b = 3.785$ Å, $c = 9.512$ Å, $d_{ap} = 1.980$ Å, $d_{eq} = 1.934$ Å, $2\theta = 156.233°$. The

results imply that our calculation methods are reasonable, and the calculated results are authentic.

We analyzed the relative degree of difficulty for different ions doping into anatase $TiO_2$ by impurity formation energies, which is a widely accepted method. In this work, the impurity formation energy is defined as the following formula[16]:

$$E_f = E_{TiO_2:D} - E_{TiO_2} - \frac{1}{2}E_{N_2} - E_{Yb} + \frac{1}{2}E_{O_2} + E_{Ti}, \quad (1)$$

where $E_{TiO_2:D}$ and $E_{TiO_2}$ are the total energy of N+Yb-doped $TiO_2$ and pure $TiO_2$ in the same size supercell. $E_{N_2}$ and $E_{O_2}$ are the energy of $N_2$ and $O_2$ gas molecular, $E_{Yb}$ and $E_{Ti}$ are the energy of bulk Yb and Ti metal, respectively. The calculated results are shown in Table 1. According to the results, $E_f$ of N+Yb-doped $TiO_2$ is larger than others. As a consequence, the synthesis of the N+Yb-doped $TiO_2$ becomes relatively difficult in the experiment because much larger formation energy is required. In addition, the lattice distortions, average bond lengths, average net charges by Mulliken population analysis and average octahedral dipole moments in different ions doped anatase $TiO_2$ by geometry optimizing are given in Table 1. From the table, compared with that of pure $TiO_2$, the length of the Ti-O bonds are longer in different ions doped anatase $TiO_2$, and the cell volumes are bigger. The average net charges on atoms are different. The changes of cell volume, bond length and charge on atoms result in the center of gravity of negative electric charges would be deviated from the position of $Ti^{4+}$ ion in $TiO_6$ octahedron and its dipole moment would not still be zero. According to the results of geometry optimization, the atom positions and net charges can be obtained. Then, we can get the center of gravity of six O ions in $TiO_6$ octahedron, and the distance between the center of O ion and Ti ion can be cal-
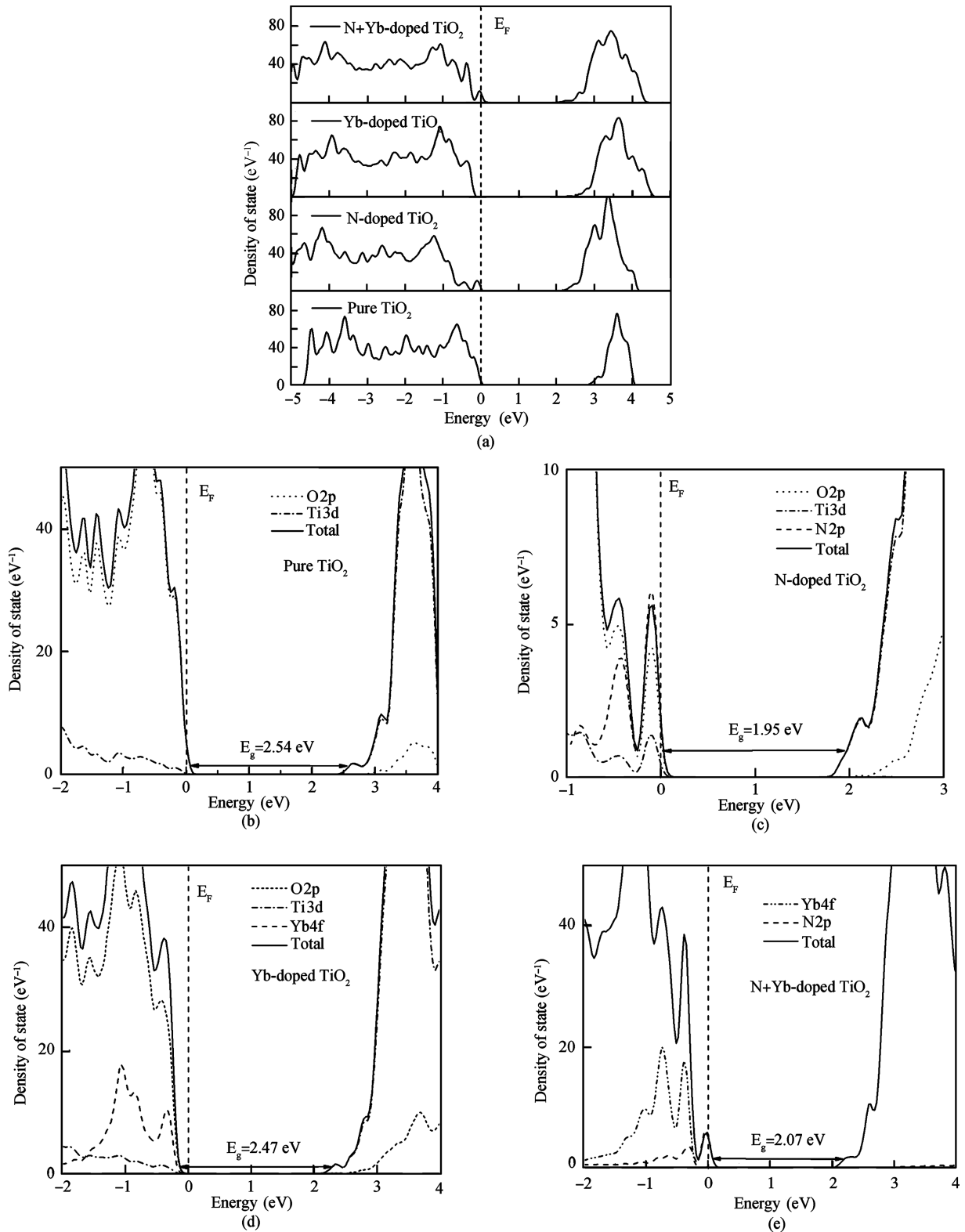
Fig. 3. (a) Calculated and comparison TDOS of different ions doped $TiO_2$. Calculated PDOS of (b) pure $TiO_2$, (c) N-doped $TiO_2$, (d) Yb-doped $TiO_2$, (e) N+Yb-doped $TiO_2$ around the band gap.

culated. Thus, the $TiO_6$ dipole moment will be obtained by using the dipole moment formula ($\mu = qr$, where $q$ is the net charge, and $r$ is the distance between the center of O ion and Ti ion). The dipole moment of distorted octahedral can occur the local internal fields which are beneficial to the separation of photoexcited electrons and holes, and are useful for enhanc-

ing photocatalytic activity[17]. According to Table 1, N doping or Yb doping can greatly enhance the photocatalytic activity of $TiO_2$. This conclusion is consistent with the results in recent literature[18]. For N+Yb-doped $TiO_2$, these changes are more obvious than that of N doping or Pr doping $TiO_2$. This means that N+Pr-doping can further enhance the photocatalytic activ-

ity of TiO$_2$ compared with single ion doping.

## 3.2. Electronic structure and optical properties

Figure 2 shows the band structure of pure TiO$_2$ along the highest symmetrical direction of the first Brillouim zone. The calculated band gap is 2.54 eV, which is less than the experimental value of $E_g = 3.23$ eV due to the limitation of DFT: the discontinuity in the exchange-correlation potential is not taken into account within the framework of DFT[19]. From Fig. 2, the conduction band minimum (CBM) is located at G, and the energy of the valence band maximum (VBM) is very closed to G; the VBM is located at G approximately. So the anatase TiO$_2$ can be seen as direct band gap semiconductor[20].

For further analyzing the constitution of VB and CB and understanding the change of electronic structures brought by doping, the calculated total density of states (TDOS) and partial density of states (PDOS) (as depicted in Figs. 3(a) to 3(e)) are inspected. In the pure TiO$_2$, VB and CB consist of both the O2p states and Ti3d states, but VB is dominated by O2p states and CB by Ti3d states. It is clear that the VB of N-doped TiO$_2$ is formed mainly by the O2p states and Ti3d states, the CB is consisted mainly by Ti3d states, the VB is formed by hybridization of O2p states with N2p states, and the impurity energy levels located above the VBM are formed by N2p states, which overlap with VBM. If the impurity energy levels are taken into account, the band gap of N-doped is narrowed to 1.95 eV. N-doped form shallow acceptor[21], which can reduce the recombination rate of charge carriers and thus improve the photocatalytic activity of TiO$_2$. The electrons in the VB can be excited to the impurity energy levels and then subsequently be excited to the CB by absorption of visible light due to the formation of impurity energy levels. For Yb-doped TiO$_2$, the impurity energy levels formed by Yb4f states are sufficiently mixed with the VB top of TiO$_2$, so the VB is broadened, and the band gap of Yb-doped is narrowed to 2.47 eV. For N+Yb-doped TiO$_2$, the impurity energy levels located above the VBM are formed by N2p states, and the impurity energy levels located at the top of the VB are formed by Yb4f states. The band gap of N+Yb-doped is narrowed to 2.07 eV. These kinds of impurity energy levels can act as trap centre for photoexcited electrons, which can reduce the recombination rate of charge carriers and thus improve the photocatalytic activity of TiO$_2$. The VB width ($-5.02$ to 0.07 eV) of N+Yb-doped is 5.09 eV, and the VB width ($-5.16$ to $-0.02$ eV) of N-doped TiO$_2$ is 5.14 eV. Compared with that of N+Yb-doped, we can see the VB width of N-doped is broadened, and the VBM shift much downward 0.09 eV. For the CBM of N+Yb-doped and N-doped, one is located at 2.14 eV, the other is at 1.93 eV, and the CBM of N-doped shift much downward 0.21 eV. As a result, the band gap of N+Yb-doped is 0.12 eV more than the band gap of N-doped.

On the basis of the electronic band structure, the optical absorption spectra of pure polycrystalline anatase TiO$_2$ between 300 and 1100 nm are calculated. The results are shown in Fig. 4. For these calculations, the scissors operator applied is 0.69 eV, accounting for the difference between the experimental band gap (3.23 eV) and the calculated band gap (2.54 eV). From Fig. 4, compared with pure TiO$_2$, the fundamental absorption edge red-shifts toward visible-light region obviously by N doping TiO$_2$. The reason is that the band gap of N-doped is narrowed obviously, so the electrons in the VB can be excited to
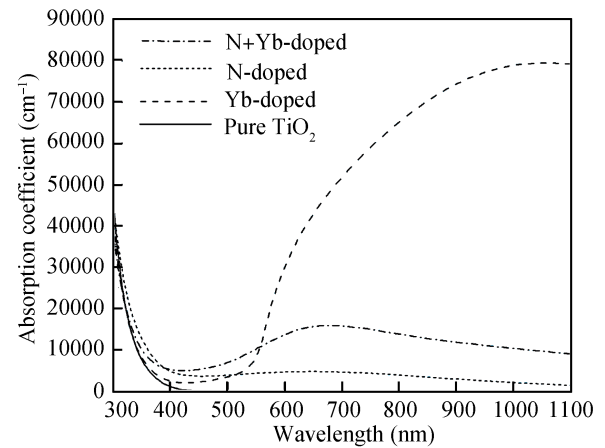


Fig. 4. Optical absorption curves of calculated for various types ion-doped TiO$_2$.

the CB by absorption of visible light. For Yb-doped, the fundamental absorption edge also red-shifts toward the visible-light region. In particularly, there is great absorption coefficient in the visible-light region. The obviously absorption properties in the IR part is due to the transition between $^2F_{7/2}$ and $^2F_{5/2}$[22]. For N+Pr-doped, the fundamental absorption edge is obviously red-shift than that of Yb-doped, and there is also great absorption coefficient in visible-light region. The distance between the impurity energy levels and OP$_\pi$ states is small[23], the absorption coefficient in visible-light region is due to the electrons transition between OP$_\pi$ states and Yb4f states.

## 3.3. Edge position

The ability of a semiconductor which undergoes photoexcited electron transfer to adsorbed species on its surface is governed by its band energy position and the redox potentials of the adsorbate. The acceptor and donor are the species absorbed on the semiconductor surface which need to be reduced by the electrons and to be oxidized by the holes, respectively. If the potential of the acceptor species absorbed on the semiconductor surface is lower (more positive) than the CB potential of the semiconductor, it can be reduced by the electrons in the CB. Also, if the potential of the donor species needs to be higher (more negative) than the VB potential of the semiconductor, it can be oxidized by the holes in the VB[24,25]. In order to study the changes of the photocatalytic activity of different ions doped TiO$_2$, we calculated the band edges position of N-doped, Yb-doped and N+Yb-doped, respectively. Here in the electronegativity of an atom is the arithmetic mean of the atomic electron affinity and the first ionization energy, other than the common-defined term. The CB edge position of a semiconductor at the point of zero charge can be expressed empirically by[26,27]:

$$E_{CB} = X - E^e - 0.5E_g, \qquad (2)$$

where $E_{CB}$ is the CB edge potential, $X$ is the electronegativity of the semiconductor which is the geometric mean of the electronegativity of the constituent atoms. $E^e$ is the energy of free electrons on the hydrogen scale ($\approx 4.5$ eV), and $E_g$ is the band gap energy of the semiconductor. According to this expression, the rough CB edge potential of TiO$_2$ is $-0.303$ eV with respect
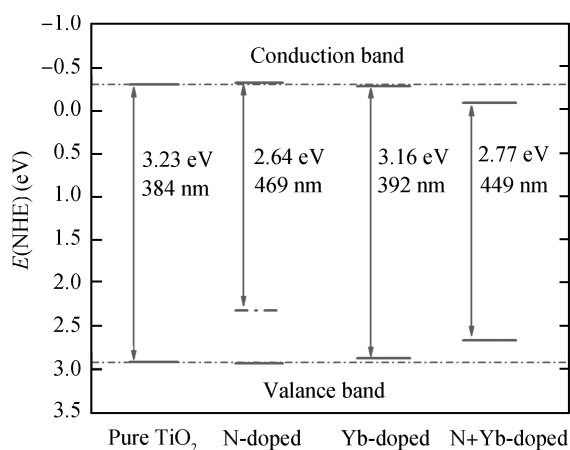
Fig. 5. Calculated band energy position of different ions doped TiO$_2$. The band gaps and corresponding wavelength threshold were corrected by "scissors operator" in this figure.

to the normal hydrogen electrode. Subsequently the edge position of the VB of the photocatalyst is determined as 2.927 eV based on its band gap energy. This result is very consistent with the band energy position of TiO$_2$ in Ref. [25]. In Fig. 5, we plot the band energy position of different ions doped TiO$_2$. It is well known that H$_2$O$_2$ and O$_3$ can oxide many organics because they have strong oxidative potential 1.77 eV (H$_2$O$_2$) and 2.07 eV (O$_3$). Compared with that of H$_2$O$_2$ and O$_3$, the oxidative potential of VB is 2.927 eV, so the holes in the VB of TiO$_2$ have stronger oxidation potential. Compared with H$_2$O$_2$ and O$_3$, N-doped and Yb-doped TiO$_2$ photocatalysts have excellent redox ability. However, compared with that of pure TiO$_2$, the CB edge is slightly downward shifted, and the VB edge is slightly upper shifted for N+Yb-doped; the change is not obvious, which means that the photocatalytic activity of N+Yb-doped TiO$_2$ photocatalysts is still excellent.

## 4. Conclusion

In this paper, the crystal structures, electronic structures and optical properties of N-doped, Yb-doped and N+Yb-doped anatase TiO$_2$ were studied by using the plane-wave ultrasoft pseudopotential method based on the density functional theory. The calculations show that the dipole moments of octahedral in crystal are increased due to the change of lattice parameters, bond length and charges on atoms, which is very effective for the separation of photogenerated electron-hole pairs and the improvement of the photocatalytic activity of TiO$_2$. For N+Yb-doped TiO$_2$, the impurity energy levels could act as shallow acceptor, which can reduce the recombination rate of charge carriers and thus improve the photocatalytic activity of TiO$_2$. Yb-doped and N+Yb-doped TiO$_2$ manifest greater absorption coefficients in visible-light region due to the interband transition between OP$_\pi$ states and Yb4f states. According to the results of the band edge position, compared with that of pure TiO$_2$, the CB edge is slightly downward shifting, and the VB edge is slightly upper shifting for N+Yb-doped, the change is not obvious, it means that the photocatalytic activity of N+Yb-

doped TiO$_2$ photocatalysts is still excellent.

## References

[1] Choi W, Termin A, Hoffmann M R. The role of metal ion dopants in quantumsized TiO$_2$: correlation between photoreactivity and charge carrier recombination dynamics. J Phys Chem, 1994, 98: 13669

[2] Jing L Q, Sun X J, Xin B F, et al. The preparation and characterization of La doped TiO$_2$ nanoparticles and their photocatalytic activity. J Solid State Chem, 2004, 177: 3375

[3] Asahi R, Morikawa T, Ohwakl T, et al. Visible-light photocatalysis in nitrogen-doped titanium oxides. Science, 2001, 293: 269

[4] Anpo M, Takeuchi M. The design and development of highly reactive titanium oxide photocatalysts operating under visible light irradiation. J Catal, 2003, 216: 505

[5] Sukharev V, Kershaw R. Concerning the role of oxygen in photocatalytic decomposition of salicylic acid in water. J Photochem Photobiol A: Chem, 1996, 98: 165

[6] Jiang D, Xu Y, Hou B, et al. Synthesis of visible light-activated TiO$_2$ photocatalyst via surface organic modification. J Solid State Chem, 2007, 180: 1787

[7] Shi J W, Zheng J T, Wu P. Preparation, characterization and photocatalytic activities of holmium-doped titanium dioxide nanoparticles. Journal of Hazardous Materials, 2009, 161: 416

[8] Sasikala R, Sudarsan V, Sudakar C, et al. Enhance photocatalytic hydrogen evolution over nanometer sized Sn and Eu doped titanium oxide. International Journal of Hydrogen Energy, 2008, 33: 4966

[9] Xu J J, Ao Y H, Fu D G, et al. A simple route for the preparation of Eu, N-codoped TiO$_2$ nanoparticles with enhanced visible light-induced photocatalytic activity. J Colloid Interface Sci, 2008: 14278

[10] Liu Z Q, Zhou Y P, Li Z H, et al. Preparation and characterization of (metal, nitrogen)-codoped TiO$_2$ by TiCl$_4$ sol-gel auto-igniting synthesis. Rare Metals, 2007, 26: 263

[11] Zhao Zongyan, Liu Qingju, Zhu Zhongqi, et al. Effects of S doping on electronic structures and photocatalytic properties of anatase TiO$_2$. Acta Phys Sin, 2008, 57: 3760 (in Chinese)

[12] Xu Ling, Tang Chaoqun, Dai Lei, et al. First-principles study of the electronic structure of N-doping anatase TiO$_2$. Acta Phys Sin, 2007, 56: 1048 (in Chinese)

[13] Yan Y F, Li J B, Wei S H, et al. Possible approach to overcome the doping asymmetry in wideband gap semiconductors. Phys Rev Lett, 2007, 98: 135506

[14] Li J B, Carrier P, Wei S H, et al. Mutual passivation of donors and isovalent nitrogen in GaAs. Phys Rev Lett, 2006, 96: 035505

[15] Burdett J K, Hughbanks T, Miller G J, et al. Structure-electronic relationship of the rutile and anatase polymorphs of titanium dioxide at 15 and 295 K. J Am Chem Soc, 1987, 109: 3639

[16] Cui X Y, Medvedeva J E, Delley B, et al. Role of embedded clustering in dilute magnetic semiconductors: Cr doped GaN. Phys Rev Lett, 2005, 95: 256404

[17] Sato J, Kobayashi H, Inoue Y. Photocatalytic activity for water decomposition of indates with octahedrally coordinated d$^{10}$ configuration. II. roles of geometric and electronic structures. J Phys Chem B, 2003, 107: 7970

[18] Long N C, Cai W M, Wang Z P, et al. Correlation of electronic structures and crystal structure with photocatalytic properties of

undoped, N-doped and I-doped $TiO_2$. Chem Phys Lett, 2006, 420: 71

[19] Perdew J P, Levg M. Physical content of the exact Kohn-Sham orbital energies: band gaps and derivative discontinuities. Phys Rev Lett, 1983, 51: 1884

[20] Minoura H, Nasu M, Takahashi Y. Comparative studies of photo-electrochemical behavior of rutile and anatase electrodes prepared by OMCVD technique. Berichte der Bunsen-Gesellschaft, 1985, 89(10): 1064

[21] Li J B, Wei S H, Li S S, et al. Design of shallow acceptors in ZnO: first-principles band-structure calculations. Phys Rev B. 2006, 74: 081201

[22] Wang Xiaodan, Zhao Zhiwei, Xu Xiaodong, et al. Spectra analysis of Yb: $Y_3Al_5O_{12}$ crystals with different Yb doping concentration. Acta Phys Sin, 2006, 55: 4358 (in Chinese)

[23] Asahi R, Taga Y, Mannstadt W, et al. Electronic and optical properties of anatase $TiO_2$. Phys Rev B, 2000, 61: 7459

[24] Gai Y Q, Li J B, Li S S, et al. Design of narrow-gap $TiO_2$: a passivated codoping approach for enhanced photoelectrochemical activity. Phys Rev Lett, 2009, 102: 036402

[25] Linsebigler A L, Lu G Q, Yates J T. Photocatalysis on $TiO_2$ surfaces: principles, mechanisms, and selected results. Chem Rev, 1995, 95: 735

[26] Tang J W, Ye J H. Photocatalytic and photophysical properties of visible-light-driven photocatalyst $ZnBi_{12}O_{20}$. Chem Phys Lett, 2005, 410: 104

[27] Morrison S R. Electronchemistry at semiconductor and oxidized metal electrodes. New York: Plenum Press, 1980